Integrated Design and Analysis of Diamond-coated Drills

Chao Miao[1], Feng Qin[2], Greg Sthur[3], Kevin Chou[4] and Raymond Thompson[5]

[1]The University of Alabama, cmiao@bama.ua.edu
[2]The University of Alabama, fqin@bama.ua.edu
[3]The University of Alabama, gsthur@bama.ua.edu
[4]The University of Alabama, kchou@eng.ua.edu
[5]Vista Engineering, Inc., rthompson@vistaeng.com

ABSTRACT

The objective of this paper is to investigate the drill geometry effects on the deposition residual stresses in diamond coated carbide drills, especially the interface stresses. The approaches include (1) solid modeling of diamond-coated two-flute twist drills using commercial computer-aided design (CAD) software, and (2) finite element analysis (FEA) to simulate residual stresses in a diamond-coated drill, which are generated during the deposition process due to the mismatched thermal expansion coefficients. It is noted that the residual stresses generated by deposition in diamond-coated drills can be significant, on the order of GPa. The modeling methodology is employed to design drills of different geometries. Further, to compare interface stresses around the cutting edge, 2D FEA is applied to simulate residual stresses of the drill cross-sections and the interface stress data at the drill cutting edge is transformed to quantitatively evaluate the drill geometry effects. The major results are summarized as follows. (1) The micro-level geometry such as the edge radius has the most dominant effects on the interface stresses by the deposition. (2) In particular, the radial normal stresses can become largely tensile, over 1.0 GPa, which may affect the coating adhesion integrity. (3) Changing the macro-level geometry such as the helix angle, point angle, and web-thickness will affect the wedge angle, 10° to 20° differences, at the drill tip. However, the effects on the interface stress magnitudes are rather minor.

1. INTRODUCTION

Drilling is among the most difficult machining processes because of chip-flow restrictions, poor heat dissipation, and rapid wear, which severely limits the productivity. Drilling constitutes about 40% of all metal-cutting operations [9], and 50 to 70% of all production time is spent on making holes [1].Twist drills used for hole making probably have one of the most complex shapes in machining tooling. A standard two-flute twist drill has a configuration shown below, Fig. 1(a), which includes spiral flutes running along a cylindrical body and the point (drill tip) area. For the drill geometry study, it can be dated back to the mid-20th century. Several research groups developed drill models to formulate mathematical equations that describe the drill geometry, some relying on computer software to generate the drill model. Galloway [7] initiated the drill geometry study with the focus on the drilling process mechanics, by which the author developed analytical equations relating the point shape of a

two-flute twist drill to the geometry of the grinding cone that is used to generate the flute shape and tip area. Following the work of Galloway, Fujii et al. [5,6] developed a method to create a drill by using CAD software. In their work, the orthogonal and oblique cutting planes were defined to conduct the geometric analysis of the drill point and the cutting angles were also defined. Drills have a complex geometry, and designing an accurate drill tool based on the actual manufacturing parameters presents a challenge. Tsai and Wu [16] presented the formula describing the ellipsoidal and hyperboloidal drills in addition to the conventional drills. Further, the grinding parameter effects on the cutting angles were studied. Ehmann [4] presented an approach for the inverse problem of the manufacture of drill flutes and developed the analytical equation to form the grinding wheel profile used to generate the flute cross-section. The comparison between the analytical results and actual measured cutting angles of drill examples indicated that the average error is less than 5%. Ren and Ni [13] studied both the drill cutting angles and the flute surface models. They developed a new mathematical model to describe the drill flute and the drill flank face with a quadratic model illustrated according to the grinding parameters. Drill angles in a two-flute drill and its grinding parameters were related via vector analysis. Shyu [15] performed FEA simulations of drilling process and developed drill meshing. Choi et al. [2] created an applet to generate the meshing of multi-flute drills. Vijayaraghavan and Dornfeld [17] developed a modeling algorithm for two-flute twist drills based on CAD software. Their work ensures that the models created are of practical usage to subsequent finite element simulations of the drilling process. Their drill CAD models are defined based on the actual fabrication processes.
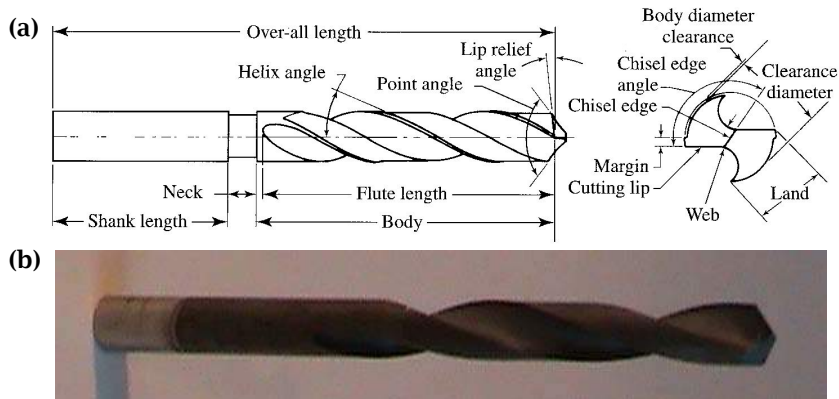

Fig.1:(a) Configuration of a standard two-flute twist drill[14] and (b) an actual twist drill.

Recently, diamond coatings using chemical vapor deposition (CVD) technologies have been applied for tooling applications to enhance machining performance. Cutting tools coated with diamond, 5 to 30 µm, can have a tool life over 50 times longer than uncoated plain tungsten-carbide (WC) tools [12]. One of the challenges in coating diamond on carbide tooling is residual stresses generated in the tool after depositions due to the largely mismatched thermal expansion coefficients between diamond and carbide [10]. The deposition residual stresses affect the adhesion quality of the diamond film and impact the cutting tool life which is mostly limited by coating delamination [11]. Diamond-coated drills have a potential for high performance drilling and for drilling of difficult-to-machine materials. Applying diamond coating on complex-shaped tooling such as drills has also been attempted, however, there is little study reported [3]. Moreover, deposition residual stresses in diamond-coated carbide drills have not been investigated before. It is also known that around any geometric changes, stress distributions will be altered and stress concentration can be significant around the substrate edge compared to the uniform coating area. Since drills have a very complex sharp, drill geometry is expected to have strong interactions with the deposition stresses. To effectively use diamond-coated drills, it is necessary to integrate the design and stress analysis from the drill geometry aspect.

In this study, a method to generate diamond-coated two-flute twist drills was developed using commercial CAD software. FEA software was further applied to simulate 3D deposition residual stresses in a diamond-coated drill. Further, 2DFEA stress simulations of drill cross-sections at the

cutting edge, at different locations, were approximated to obtain stress distributions around the cutting edge which can be extracted and transformed to quantitatively evaluate local interface stresses of different components. The solid modeling methodology was also employed to develop drill models with different geometry parameters such as the helix angle, point angle, and web thickness, and the models were further used for 2D residual stress simulations. Therefore, drill geometry effects including the cutting edge radius on the deposition stresses were quantified.

2. SOLID MODELING OF 3D DIAMOND-COATED TWO-FLUTE TWIST DRILLS

Solid modeling of a twist drill consists of several procedures. With Solidworks used in this study, first, a helix curve with a specified helix angle (later serving as the sweep trajectory) is defined. Then, the spline curve of the flute cross-section is constructed according to the mathematical representation of specific drill geometry [17]. Once the flute cross-section (spline as well as the circular portion) is completed, the sweeping function is used to create the drill flute body. Next, the left and right grinding cones are defined mimicking the fabrication process that generates the drill tip: two cutting lips and a chisel edge. Finally, an edge radius is incorporated along the cutting lips and chisel edge.

In order to model diamond-coated drills, the drill model developed above serves as the substrate and revolve-cut and shell functions are employed to generate the coating with a given coating thickness and an edge radius. The completed drill substrate and coating models can then be assembled, assuming a rigid interface, to obtain a diamond-coated twist drill.Fig.2below shows an example of solid models of a twist drill body and a diamond-coated drill.
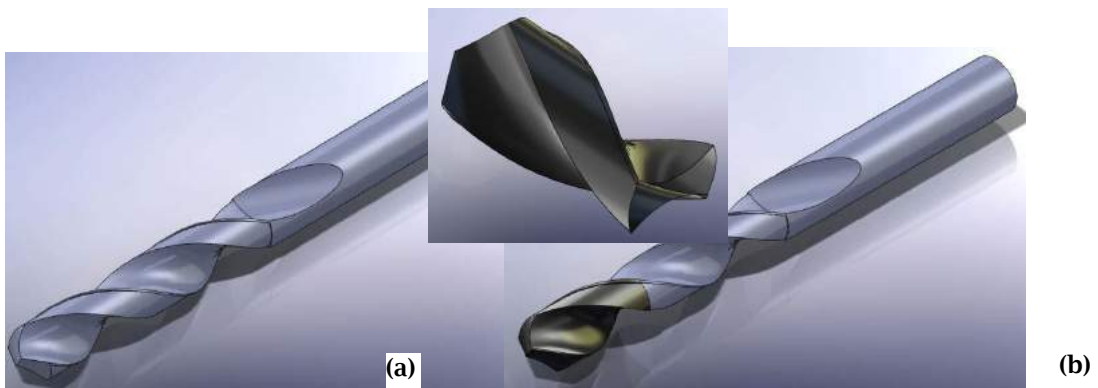

(a)

(b)

Fig. 2: An example of (a) fully defined twist drill solid model and (b) diamond coated twist drill.

3. FINITE ELEMENT ANALYSIS OF DEPOSITION STRESSES

3.1 3D Drill Stress Analysis

Due to the mismatched thermal expansions between the drill substrate (WC) and coating (diamond), residual stresses will be developed in the diamond-coated drill when the deposition process is completed and the drill is returned to room temperature. To conduct 3D deposition-stress simulations, the drill substrate and coating model files from Solidworks are imported into FEA software, ABAQUS, for assembly and merging. Meshing is then performed using the element type C3D4 free Tet elements and the coating area receives finer meshing. For the meshed model, the cutting-lip and chisel edge areas are further refined, Fig.2 below, as high stress gradients can be expected. Moreover, the material properties for the substrate material, WC, are 620 GPa of Young's modulus, 0.22 of Poisson's ratio and 5.5 μm/(m.K) of thermal expansion coefficient. For diamond coatings, the Young's Modulus is 1200 GPa, Poisson's ratio is 0.07, and the thermal expansion coefficient is 2.5μm/(m.K).For the stress simulations, static structural analysis is conducted and a deposition temperature of 800°C is set as the initial condition and the room temperature of 25°C is defined as the final temperature. Material behaviors of both WC and diamond are assumed to be

elastic due to their high melting points and brittleness. Thus, the coating-substrate interface was considered to be rigid. The boundary condition includes a fully constrained surface at the drill bottom.
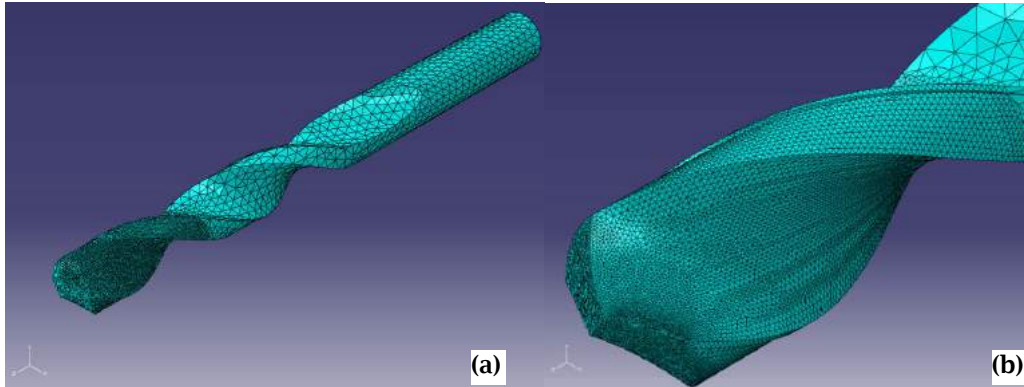

Fig.3: Element meshing for diamond-coated drill stress simulations: (a) the entire drill model and (b) around drill tip.

For the illustration purpose, below is a stress analysis example from a diamond-coated drill: 6.34 mm diameter, 34. 5 mm flute length, 30° helix angle, 135° point angle, 1.33mm web-thickness, and 3µm edge radius. The length of the coating area along the longitudinal direction is 12.7 mm. Fig. 4 shows the stress contours (longitudinal normal stress)of the coated drill. It is noted that on the coating surface with moderate curving, the longitudinal stress is in the neighborhood of ~3.0 GPa in compression. This is consistent with the results obtained from the biaxial stress analysis. On the other hand, the substrate has tensile stresses, order of 100 MPa, and generally small in the area away from the coating area. It is further noted that around the drill tip, large stress gradients are prominent. Fig. 5 plots the longitudinal stress in the sectional view of a coated drill to illustrate high stress concentrations near the drill tip, especially around the cutting edge.

It is known that interface stresses (between the coating and substrate) are more closely related to the coating integrity. Thus, it was intended to obtain the stress data along the interface. However, this is a complex and time-consuming process for the 3D drill model. Thus, 2D approximation of stress analysis, described below,was applied to attain the interface stress data for further evaluations and investigation of drill geometry effects.
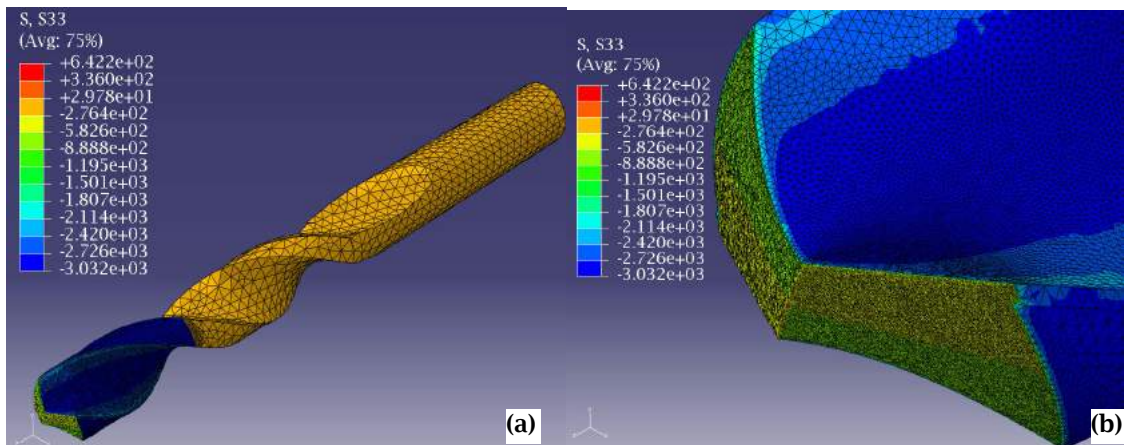

Fig.4: An example of stress distributions (longitudinal normal stress) in a diamond-coated drill: (a) overall and (b) near drill tip.
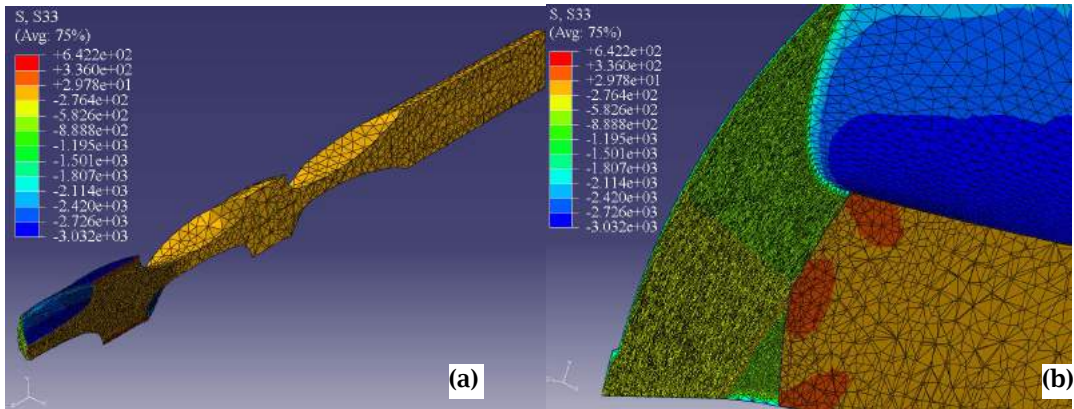
Fig. 5: Longitudinal normal stress contours in a sectional view of a diamond-coated drill: (a) overall and (b) near drill tip.

3.2 2D Approximation

In order to evaluate the drill geometry effects on the interface stresses of a diamond-coated drill, 2D drill cross-sections around the drill tip were generated at different locations, both the cutting lip and chisel edge, using a plane normal to the cutting edge. Fig.6 shows an example of a 2D drill section being generated.
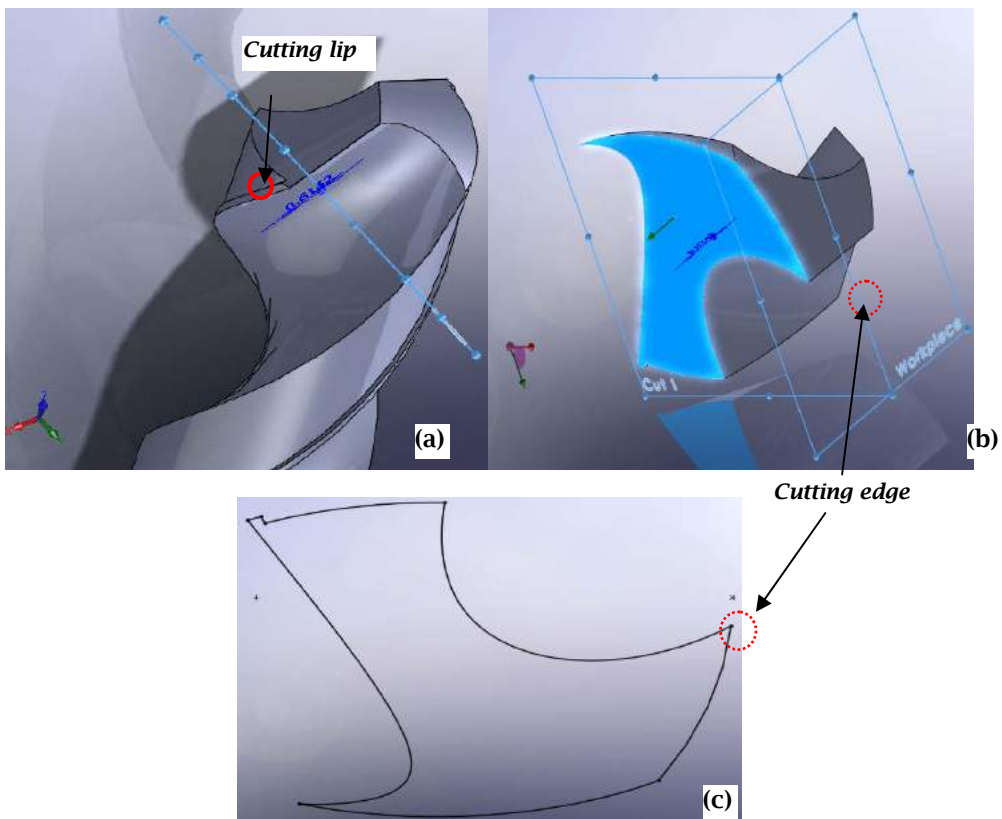

Fig. 6: An example of 2D section of a drill for FEA stress analysis: (a) Sectional plane specification, (b) Intersected profile on the drill, and (c) 2D view of the cross-section.

200

Considering the relative motion at the local drill edge (i.e., rotation, as in actual drill operation), a workpiece plane can be defined, Fig.6(b), to evaluate the cutting geometry such as the rake angle. As seen from the Fig.6(b), the highlighted area is the cross-section and the two planes represent the sectional plane and workpiece plane. In this particular cross-section, which is about 1 mm away from the outer diameter, the rake and relief angles are 30.11° and 5.8°, respectively. The cross-section profile can then be extracted and exported to ABAQUS. With addition of a specified edge radius and a coating layer, uniformly all around, 2D FEA simulations of deposition stresses is conducted, with an assumption of 2D plane strain. The material properties and the deposition temperature are the same as in the 3D analysis. The boundary conditions applied include one fully constraint corner (away from the cutting edge) and another partially constrained (one direction) point.

As an example, Fig.7 shows the maximum principal stress contours in the studied cross-section. This example is from a diamond-coated drill: 6.34 mm diameter, 34. 5 mm flute length, 30° helix angle, 135° point angle, 1.33 mm web-thickness, and 3μm edge radius. The coating is 5 μm thick. The cross-section is on the cutting lip, about 1 mm away from the outer diameter. The stresses are in the range from 2 GPa to 3 GPa. Though the stress distribution is uniform in most areas, the area around the coating-substrate interface, particularly near the cutting edge, has high stress gradients, Fig. 7(b).
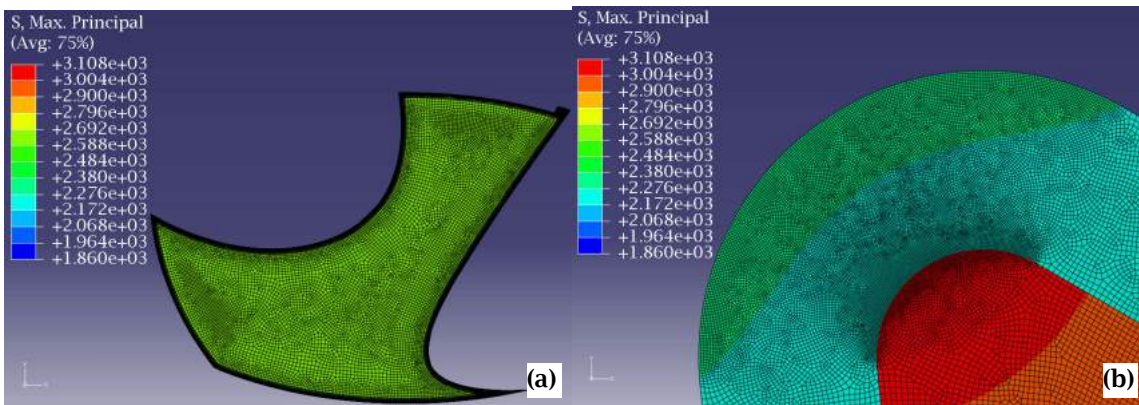

Fig. 7: Deposition stress contours(maximum principal stress) in a 2D coated-drillsection, (a) Overall distribution and (b)around the cutting edge area.

In order to quantify the interface stresses around the cutting edges, the stress data along the interface of 2D results was extracted and stress transformation was conducted using the Mohr's circle concept; The stresses in the Cartesian coordinate system in FEA were changed to stress components associated with the local polar coordinate system around the cutting edge, including 3 components, namely, the radial normal stress (σ_r), the circumferential normal stress (σ_θ), and the shear stress ($\tau_{r\theta}$). Fig. 8(a) illustrates the 3 stress components around the cutting edge, noting that they vary along the rounded curve and can be evaluated in reference to a point where the rounded edge begins.

Fig. 8(b) plots the interface stress profiles, all 3 components, for the example illustrated above. The stresses are at the coating-substrate interface and plotted around the edge (coordinate 0 is where the edge curve starts).The abscissa in the Figure is the distance normalized by the arc length of the rounded edge (Fig.8(a)). It can be seen that tensile radial normal stresses, as high as close to 1.5 GPa, are developed because of the edge sharpness. Such high tensile stresses can be detrimental in brittle fracture due to crack propagations and require greater adhesion strengths. On the other hand, the circumferential stresses are in the neighborhood of 3 GPa in compression. The large compressive tangential stresses have been viewed to be beneficial for abrasive wear rate reductions, however, buckling could be another mechanism risky to the coating failure [8]. The shear stresses are in the range of ±0.6 GPa.
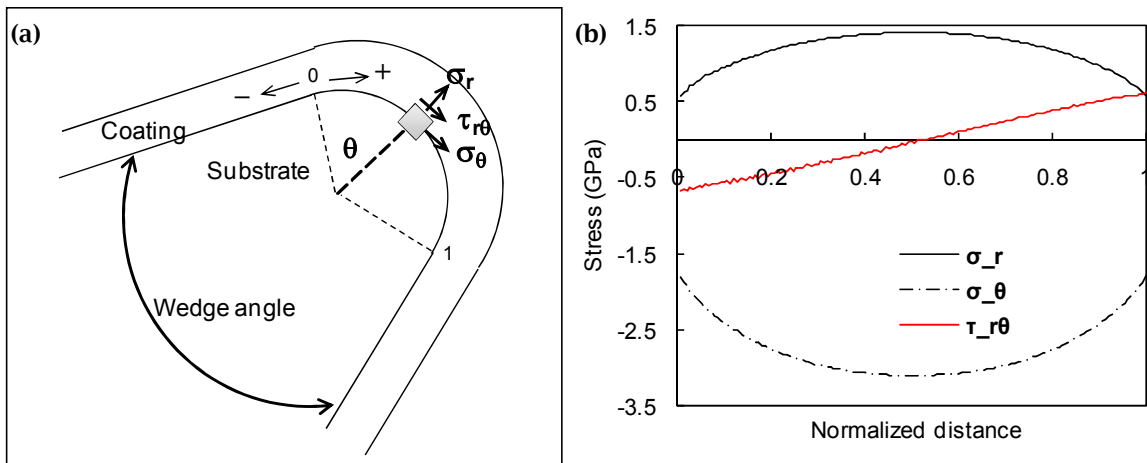
Fig.8:(a) A schematic drawing showing the interfacial stress components around the edge area, and (b) Interface stress profiles around the cutting edge of a diamond-coated drill cross-section.

3.3 Drill Geometry Effects

Using the developed modeling methodology, the CAD program was applied to design twist drills with different geometries. Among drill geometry parameters, the helix angle, the point angle, and the web thickness are considered as the major parameters to be investigated [14]. These parameters affect the cutting geometry, mainly the rake angle, and thus, the drilling process. In addition, the wedge angle changed may possibly affect the deposition stresses, the studied subject of this paper. In this study, the helix angles tested were 20°, 30°, and 40°, and the point angles included 90°, 118°, and 135°. The web-thicknesses changed from 0.64 mm, to 1.3 mm and 1.9 mm. Fig. 9 and Fig.10 are examples of twist drills with different helix and point angles, respectively. Moreover, the micro-level of drill geometry, namely, cutting edge radius, was investigated as well. Three levels of edge radii were simulated: 3 μm, 7 μm, and 15 μm.
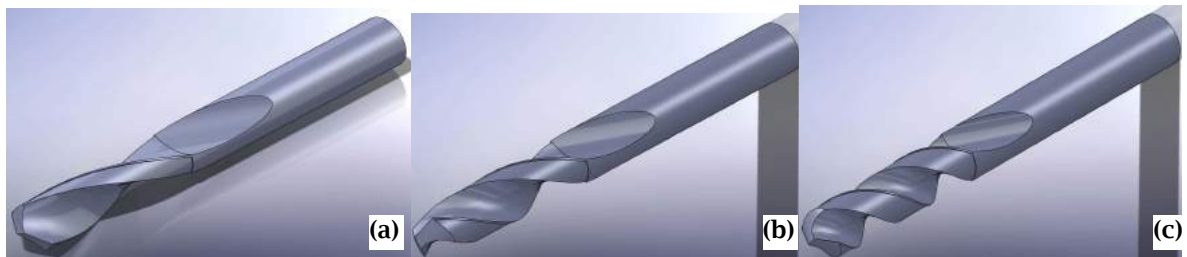

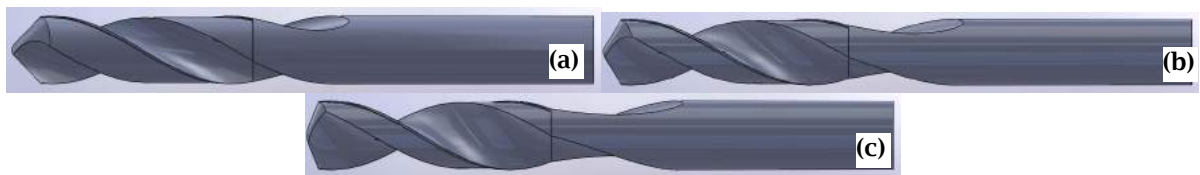Fig.9: Drills with different helix angles: (a) 20°, (b) 30°, and (c) 40°.

Fig.10: Drills with different point angles: (a) 90°, (b) 118°, and (c) 135°.

Applying the same procedures defined earlier, different 2D cross-sections along the drill cutting lip and chisel edge, at 3 different locations (Fig. 11 below), were obtained for further stress analysis. The

wedge angle of each section was also evaluated and compared between different types of drills. Tab.1 below lists the wedge angles a different cross-sections of drills with different helix and point angles.

Point angle (°)	Sec.1	Sec. 2	Chisel Sec.	Helix angle(°)	Sec.1	Sec.2	Chisel Sec.
90	47	53	90	20	65	68	113
118	54	59	114	30	54	59	113
135	57	61	129	40	43	49	113

Tab. 1: Wedge angle (°) at different sections of drills with different point and helix angles.
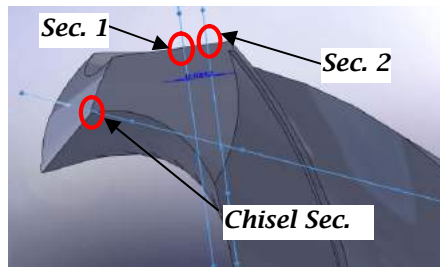

Fig. 11: Locations of different drill cross-sections analyzed in Tab. 1.

Further, a layer of diamond coating with a given thickness was added to the drill cross-section, uniformly all around. Then, FEA deposition stress analysis was conducted to all generated diamond-coated sections according to the simulations specified earlier. Then, the stress data along the interface was extracted and transformed to evaluate the interface stress profiles. Fig.12 shows the helix angle effects on the radial normal stresses. It is noted that the radial normal stresses are virtually not affected by the helix angle. Note that the wedge angle, formed by the rake and relief angles, changed due to different helix angles is fairly noticeable, 10° to 20° differences, but the effect on the deposition stresses is little. On the other hand, Fig.13 plots the normal stress components affected by the drill cutting edge radius. It is clearly noted that the edge radius (r_e) significantly modifies the deposition interface stresses. For the radial normal stress (σ_r), the maximum reduces from 1.4 GPa for 3 µm r_e to 0.7 GPa for 15 µm r_e. The large edge radius also shows smooth stress gradients along the edge. For the circumferential normal stress (σ_θ), stress reductions by the edge hone were from -3.0 GPa for 3 µm r_e to -2.7 GPa for 15 µm r_e. For the shear stress component ($\tau_{r\theta}$), the stress magnitude is smaller and reductions at a large radius are also evident: from ~0.7 GPa for 3µm r_e to ~0.3 GPa for 15 µm r_e.
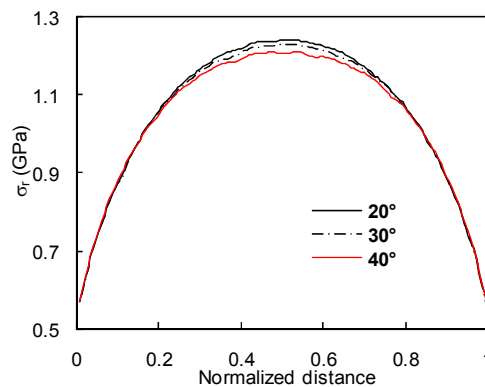

Fig. 12: Interface stress profiles, radial normal component, for drills of different helix angles.
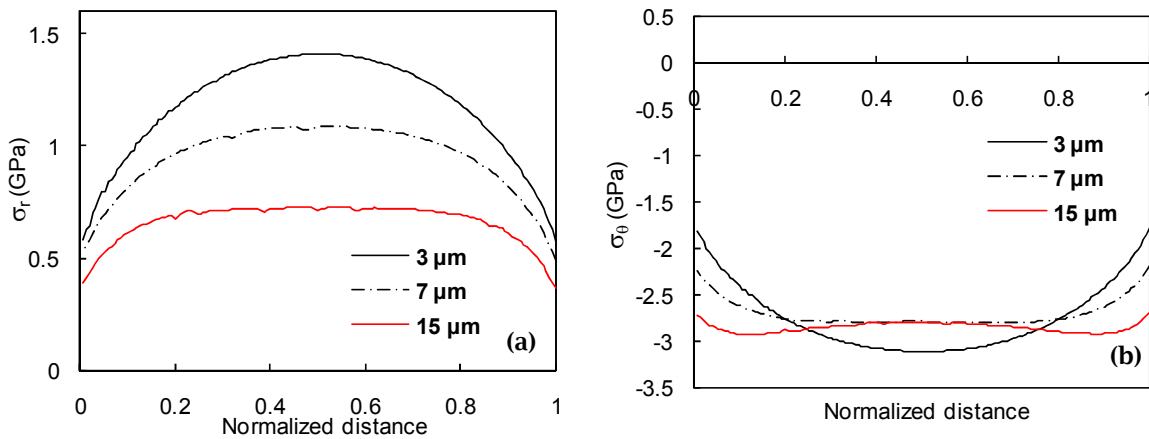
Fig.13: Edge radius effects on interface stress profiles of diamond-coated drills: (a) radial normal stress, and (b) circumferential normal stress.

In order to reach quantitative conclusions, the maximum values of stress magnitudes of all 3 components were obtained to examine the drill parameter effects studied. Tab. 2, Tab. 3, , Tab. 4, and Tab. 5 below compare the edge radius, helix angle, point angle, and web-thickness effects, respectively, on the maximum interface stresses by deposition. It is clear that the smallest edge radius drill, i.e.,3µm, has the largest $\sigma_{rmax}$and $\sigma_{\theta max}$, 1.41GPaand3.11GPa,respectively. For the drill with15 µm edge radius, it has the σ_{rmax}=0.73 GPaand$\sigma_{\theta max}$=2.94 GPa, respectively. On the other hand, the macro-level parameters of drill geometry do not affect the deposition stress magnitudes.

Edge Radius(µm)	3µm	7µm	15µm
$\sigma_{rmax}(GPa)$	1.41	1.08	0.73
$\sigma_{\theta max}(GPa)$	3.11	2.80	2.94

Tab. 2: Maximum interface normal stresses for different edge radii.

Helical angle (°)	20	30	40
$\sigma_{rmax}(GPa)$	1.24	1.23	1.21
$\sigma_{\theta max}(GPa)$	3.05	2.89	2.73

Tab. 3: Maximum interface normal stresses for different helix angles.

Point angle(°)	90	118	135
$\sigma_{rmax}(GPa)$	1.217	1.227	1.234
$\sigma_{\theta max}(GPa)$	2.78	2.89	2.94

Tab. 4: Maximum interface normal stresses for different point angles.

Webthickness(mm)	0.635	1.33	1.91
$\sigma_{rmax}(GPa)$	1.22	1.23	1.23

$\sigma_{\theta max}(GPa)$	2.85	2.89	2.92

Tab. 5: Maximum interface normal stresses for different web thicknesses.

4. CONCLUSIONS

Solid modeling of diamond-coated drills using CAD software has been achieved in this study. 3D FEA simulations have been developed as well to study deposition residual stresses in a diamond coated drill. The nominal longitudinal normal stresses in the area of less curvature are about 3 GPa in compression, which is consistent with the biaxial stress analysis. The model can be used to design drills with different geometric parameters. Moreover, 2D approximation of FEA stress simulations is applied to investigate drill geometry effects on interface stresses around the drill cutting edge. The residual stresses generated by deposition in the diamond-coated drills can be significant. The micro-level geometry such as the edge radius has the most dominant effects on the interface stresses. In particular, the radial normal stresses can become largely tensile, over 1.0 GPa, which may affect the adhesion integrity. Changing the macro-level geometry such as the helix angle, point angle, and web-thickness will affect the wedge angle, 10° to 20° differences, at the cutting tip. However, the effects on the interface stress magnitudes are rather minor. For future work, the coating thickness effects on the interface residual stresses in diamond coated drills will be incorporated. Moreover, during machining, the deposition residual stresses will be affected by the induced mechanical and thermal loads. Thus, it is necessary to concurrently investigate the stress field evolutions during drilling in order to effectively use diamond coated drills.

5. ACKNOWLEDGEMENTS

6. REFERENCES
[1]   Benes, J.: Hole Making Trends Run Deep, Fast, and Dry, American Machinist, (May 2000), 2000, 97–102.
[2]   Choi, J.; Min, S.; Dornfeld, D. A.; Alam, M.; Tzong, T.: Modelingof Inter-Layer Gap Formation in Drilling of a Multilayered Material, Proc. Of6th CIRP International Workshop on Modeling of Machining Operations, McMaster University, Hamilton, Canada, May 19–20, CIRP, Hamilton, Ontario,Canada, 2003, 113–118.
[3]   Chen, M.; Jian, X.G.; Sun, F.H.; Hu, B.; Liu, X.S.: Development of diamond-coated drills and their cutting performance, Journal of Materials Processing Technology, 129, 2002, 81-85.
[4]   Ehmann, K. F.: Grinding Wheel Profile Definition for the Manufactureof Drill Flutes, CIRP Ann., 39(1), 1990, 153–156.
[5]   Fujii, S.; DeVries, M. F.; Wu, S. M.: An Analysis of Drill Geometryfor Optimum Drill Design by Computer — Part I: Drill Geometry Analysis, ASME J. Eng. Ind., 92, 1970, 647–656.
[6]   Fujii, S.; DeVries, M. F.; Wu, S. M.: An Analysis of Drill Geometryfor Optimum Drill Design by Computer — Part II: Computer Aided Design, ASME J. Eng. Ind., 92, 1970, 657–666.
[7]   Galloway, D. F.: Some Experiments on the Influence of Various Factors on Drill Performance, Trans. ASME, 79, 1957, 191–231.
[8]   Gahlin, R.; Alahelisten, A.; Jacobson, S.: The effects of compressive stresses on theabrasion of diamond coatings wear, 196, 1996, 226-233.
[9]   Hamade, R. F.; Ismail, F.: A Case for Aggressive Drilling of Aluminum, Journal of Materials Processing Technology, 166, 2005, 86-97.
[10] Hu, J.; Chou, Y. K.; Thompson,R. G.: On Stress Analysis of Diamond Coating Cutting Tools, Transactions of NAMRI/SME, 35, 2007, 177-184.
[11] Hu, J.; Chou, Y. K.; Thompson, R. G.:A Numerical Study of Interface Behavior of Diamond Coated Cutting Tools, Transactions of NAMRI/SME, 36, 2008, 533-540.
[12] Oles, E. J.; Inspektor, A.; Bauer, C.E.: The New Diamond-coated Carbide Cutting Tools, Diamond and Related Materials, 5(6-8), 1996, 617-624.
[13] Ren, R.; Ni, J.: Analyses of Drill Flute and Cutting Angles, Int. J.Adv. Manuf. Technol., 15, 1999, 546–553.

[14] Stephenson, D. A.; Agapiou, J. S.: Metal Cutting Theory and Practice, CRC, 1st edition, 1996, 205-218.

[15] Shyu, B.: Computer Simulations for Burr Formation Study, Ph.D. thesis, University of California, Berkeley.

[16] Tsai, W. D.; Wu, S. M.: Computer Analysis of Drill Point Geometry, International Journal of Machine Tool Design and Research, 19(1), 1979, 95–108.

[17] Vijayaraghavan, A.; Dornfeld, D. A.: Automated Drill Modeling for Drilling Process Simulation, Journal of Computing and Information Science in Engineering, 7, 2004, 276–282.